

## Interparticle interactions in water-in-oil microemulsions: Dielectric and ir investigations

M. D'Angelo, D. Fioretto, G. Onori, and A. Santucci

*Istituto Nazionale di Fisica della Materia and Dipartimento di Fisica, Università di Perugia I-06100 Perugia, Italy*

(Received 30 October 1997; revised manuscript received 24 July 1998)

The high-frequency dielectric response of sodium bis(2-ethylhexyl)sulfosuccinate (AOT) reverse micelles in *n*-heptane has been measured in the range 0.01–20 GHz as a function of volume fraction  $\phi$  of a dispersed phase at a fixed value of the water to surfactant molar ratio  $W=11$ . A relaxation phenomenon has been observed that is connected to the AOT ion pair diffusion at the water-surfactant interface. This dielectric relaxation has been found to be markedly affected by the interparticle interactions that have been modulated by adding different amounts of NaCl. In order to reveal the connections between attractive interactions among the droplets and the stereochemical configurations of AOT molecules, an ir study has been performed on the carbonyl stretching band of AOT molecules in the micellar aggregates. A comparison with dielectric data shows that a correlation exists between the intensity of attractive interactions and the composition of AOT rotamers in the microemulsion system. These results support the hypothesis that attractive intermicellar interactions are favored by a particular orientation and packing of nonpolar tails of AOT molecules in the micellar microaggregate. [S1063-651X(98)10312-4]

PACS number(s): 82.70.-y, 77.22.Gm, 77.84.Nh, 63.50.+x

### I. INTRODUCTION

In recent papers we reported on the investigation of dielectric and ir properties of sodium bis(2-ethylhexyl)sulfosuccinate (AOT) microemulsions in *n*-heptane and  $\text{CCl}_4$  [1–3]. A dielectric dispersion was observed in the microwave region. The evolution of its dielectric parameters was examined as a function of the water to surfactant molar ratio ( $W$ ) at different volume fractions  $\phi$  of the dispersed phase (water plus AOT). In the dilute limit, the behavior of this dielectric relaxation with  $W$  was interpreted in terms of the diffusion of the surfactant ion pairs whose mobility depends on the micellar hydration degree. In particular, the relaxation process observed in the almost dehydrated reverse micelles was attributed to the rotational diffusion of the whole micellar aggregate having an almost rigid structure. As the water content inside the micellar core is increased, an increasing fraction of completely hydrated AOT ion pairs achieves enough mobility to give a separate contribution to the relaxation process. So, at the highest values of  $W$ , the dielectric relaxation was supposed to rise from the fluctuating dipole moment imparted to the microaggregate from the AOT ion pair diffusion at the water-surfactant interface.

This dielectric relaxation was found to be markedly affected by interparticle interactions. Our data, in agreement with previous results [4–6], show that interactions in these systems depend on the oil molecule size and the molar ratio  $W$  and are deeply affected by the addition of small amounts of electrolyte.

The results obtained from the previously followed experimental pathway [2,3] (change of  $W$  at a fixed value of  $\phi$ ) are difficult to interpret quantitatively since the dielectric response is connected to both interactions (depending on  $W$ ) and particle concentration (depending on both  $\phi$  and  $W$ ). In fact, increasing  $W$  at a fixed  $\phi$ , the volume of a single mi-

celle increases approximately with  $W^3$  and, as a consequence, the particle concentration correspondingly decreases.

In order to better understand the role of interactions in the dynamics of these systems, dielectric measurements have thus been performed following the easier pathway, which keeps the interaction constant at each series of measurements varying the value of  $\phi$ , at a fixed molar ratio  $W=11$ . *n*-heptane was chosen as the dispersing medium in order to enhance interactions effects [2]; different series of measurements have been carried out modulating the strength of these attractive interactions by adding different amounts of NaCl.

The microscopic origin of attractive forces in microemulsions is still not clear. A possible explanation was proposed by Lemaire, Bothorel, and Roux [5] on the basis of a mutual interpenetration of the surfactant tails. This model is consistent with the small-angle neutron scattering and light data of Huang and co-workers [4,7]. According to the model of Lemaire, Bothorel, and Roux, a strong dependence of the interaction on the packing of nonpolar tails of AOT molecules in the microaggregate is expected. It should be noticed that the proton magnetic resonance data [8–10] and ir spectra [11–13] in the carbonyl stretching region suggest that AOT molecules are present in the water in oil microemulsions as a mixture of two different rotational isomers having a different packing factor whose composition depends on different parameters such as the dispersing medium, temperature, and  $W$ . To the best of our knowledge, no studies have been performed that point out possible connections between attractive interactions among the droplets and the stereochemical configurations of AOT molecules. With this in mind, an ir study has been performed on the carbonyl stretching band of AOT molecules in micellar microaggregates to ascertain a possible correlation between the composition of AOT rotamers and intermicellar interactions as revealed by dielectric measurements.

## II. EXPERIMENT

AOT 99% (Aldrich product), purified by recrystallization from methanol and dried in vacuum, was stored in vacuum over  $P_2O_5$ . Residual water (about 0.2 mole of water per mole of AOT revealed by using a Karl Fischer titrator) has been considered as a part of the total water in the mixture. *n*-heptane 99.5% (Fluka product) was used without further purification. Deionized and bidistilled water was employed to prepare the samples; salted samples were prepared with sodium chloride 99+% (Aldrich product).

The mixtures were prepared by weight, keeping constant the molar ratio  $W=11$  and varying the volume fraction  $\phi$  of dispersed particle in the range 0.025–0.3. Five series of samples were made at different concentrations of NaCl in water, varying in the range between 0M and 0.5M.

Measurements of the complex dielectric constant have been carried out in the frequency domain using an open coaxial cell consisting of a section of a transmission line with its center abruptly terminated. The dielectric liquid to be measured fills the coaxial section of the cell and extends beyond the center conductor in the tube formed by the outer conductor of the coaxial line. The values of the real and imaginary parts of the dielectric constant were obtained from that of the complex impedance of the cell, measured by means of vectorial Network Analyzers. To this purpose, a Hewlett-Packard (HP) Model No. 8753A is used up to 3 GHz and a HP 8720C up to 20 GHz. The spurious effects introduced by the connectors and by other discontinuities were corrected by means of the calibration procedure that considers the equivalent circuit of the transmission line consisting of three impedances whose values are obtained by measuring three known materials. In our calibration procedure air, carbon tetrachloride, and iodomethane were used. For more details, see Ref. [14]. All the dielectric measurements have been performed at the fixed temperature  $T=(20.0\pm 0.1)$  °C.

ir spectra were taken at room temperature by means of a Shimadzu Model No. 470 infrared spectrophotometer equipped with a variable path-length cell and  $CaF_2$  windows. The typical path length employed was around 100  $\mu m$ .

## III. RESULTS AND DISCUSSION

### A. Dielectric measurements

Figure 1 shows the real part ( $\epsilon'$ ) of the complex dielectric permittivity of AOT/ $H_2O$ /*n*-heptane microemulsions in the range 0.001–3 GHz for some selected values of  $\phi$ . The dielectric spectrum of the most diluted samples exhibits a high-frequency dispersion region located around 100 MHz, which has been attributed to the diffusion of AOT ion pairs at the water-surfactant interface [1]. As  $\phi$  is increased, the strength of this dielectric relaxation rapidly increases and an additional dispersion appears in the low-frequency region, connected to the clustering process of microaggregates [15–17]. The contribution of this relaxation phenomenon to the high-frequency region ( $f > 10^7$  Hz) is, however, negligible. Figure 2 shows the dielectric spectrum of samples in which pure water has been replaced by a 0.5M NaCl brine. A less marked effect of the particle volume fraction on the values of  $\epsilon'$  is evidenced in addition to the absence of low-frequency

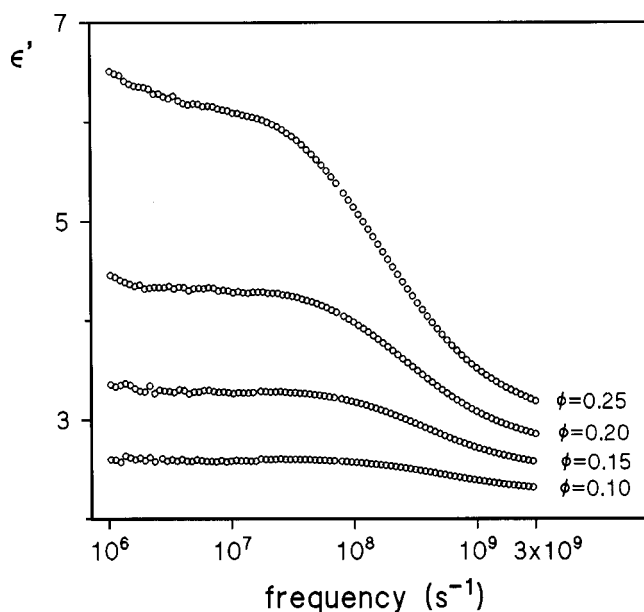


FIG. 1. Real part ( $\epsilon'$ ) of the complex dielectric permittivity of AOT/ $H_2O$ /*n*-heptane microemulsions ( $W=11$ ) for some selected values of the volume fraction  $\phi$  of the dispersed phase.

contributions to the dielectric spectrum, suggesting a negligible clustering process of microaggregates in these systems.

As an example, Fig. 3 shows the dielectric spectrum of one of the samples examined ( $\phi=0.2$ ,  $[NaCl]=0M$ ) in the frequency region 0.01–20 GHz. The frequency dependence of the complex dielectric constant was described as in previous works [1–3] in terms of the superposition of a Cole-Cole relaxation function, relative to the contribution of AOT ion pairs, located in the 100-MHz frequency region and a Debye-type function accounting for the reorientation of water mol-

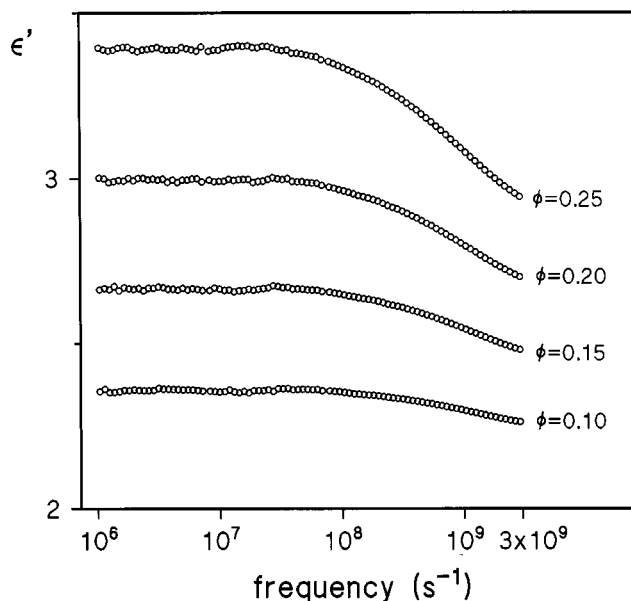


FIG. 2. Real part ( $\epsilon'$ ) of the complex dielectric permittivity of AOT/ $H_2O$ /*n*-heptane microemulsions ( $W=11$ ) for the same selected values of  $\phi$  as in Fig. 1. In these samples pure water has been replaced by a 0.5M NaCl brine.

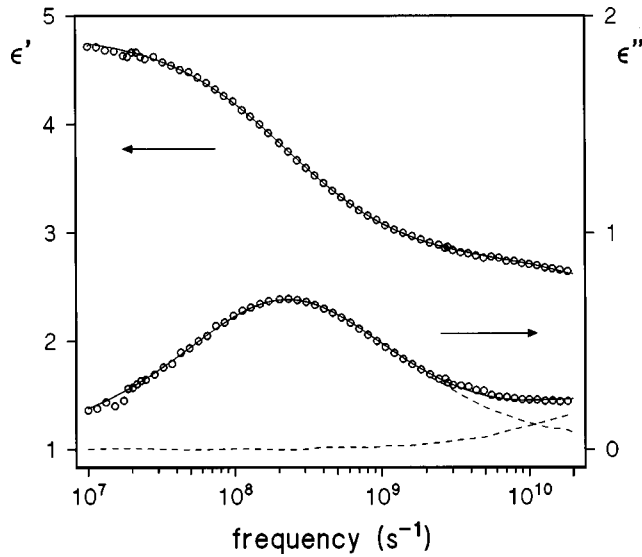


FIG. 3. Real ( $\epsilon'$ ) and imaginary ( $\epsilon''$ ) parts of the dielectric permittivity vs the frequency of AOT/H<sub>2</sub>O/*n*-heptane microemulsions ( $\phi=0.2$ ,  $W=11$ ).  $\circ$ , experimental points; —, best fit according to Eq. (1). Cole-Cole and Debye-type contributions to best fit of  $\epsilon''(\omega)$  are also shown (---).

ecules confined within the micellar core that contribute to the high-frequency part of the spectrum:

$$\epsilon^*(\omega) = \epsilon_\infty + \frac{\epsilon_1 - \epsilon_i}{1 + (i\omega\tau_1)^{1-a}} + \frac{\epsilon_i - \epsilon_\infty}{1 + i\omega\tau_2}, \quad (1)$$

where  $\epsilon_1$ ,  $\epsilon_i$ , and  $\epsilon_\infty$  are the low-, intermediate-, and high-frequency values of the complex dielectric constant, respectively,  $\omega$  is the angular frequency of the applied electric field,  $\tau_1$  and  $\tau_2$  are the relaxation times of the two processes, and  $a$  is a parameter characterizing the width of the relaxation function around  $\tau_1$ .

The interpolation procedure of the experimental data as a function of frequency was carried out by fitting the values of both the real and imaginary parts of the dielectric permittivity

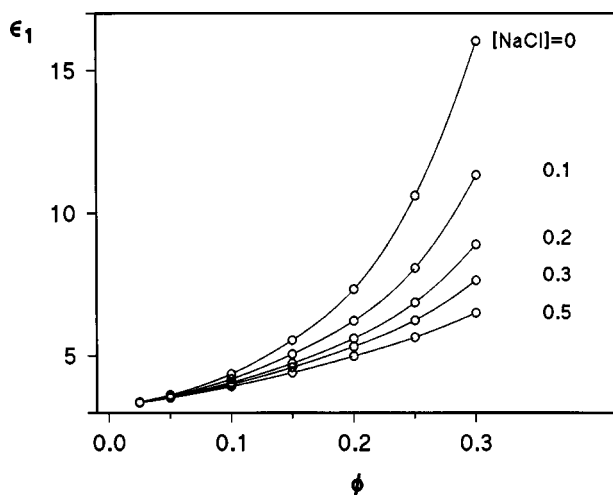


FIG. 4. Low-frequency values of the dielectric permittivity ( $\epsilon_1$ ) vs  $\phi$  for samples of microemulsions relative to different molar concentrations of NaCl brine.  $\circ$ , experimental points. Lines are a guide for the eyes.

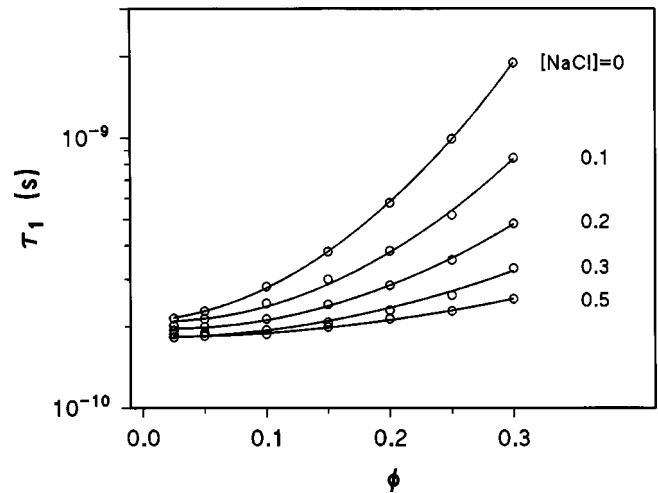


FIG. 5. Relaxation time ( $\tau_1$ ) vs  $\phi$  for samples of microemulsions relative to different concentrations of NaCl brine.  $\circ$ , experimental points; —, fitting according to Eq. (5).

ity by means of the Marquardt algorithm. The best fit curves of the experimental spectra are reported in Fig. 3 (solid lines) together with the Cole-Cole and Debye-type contributions to the best fit of the imaginary part of the dielectric permittivity [ $\epsilon''(\omega)$ ] (dashed lines). The Debye dispersion located in the region of the relaxation of bulk water is not completely contained in the available frequency window and makes only a small contribution to the spectra. The values of dielectric parameters  $\epsilon_i - \epsilon_\infty$  and  $\tau_2$  are affected by relatively large errors, making impossible the singling out of a well-defined trend in the data. A deeper discussion on the behavior of this relaxation is beyond the purpose of the present work. However, it is important to notice that the experimental values of  $\tau_2$  ( $\tau_2 \cong 6 \times 10^{-12}$  s) are lower than those of the relaxation time of bulk water ( $\tau = 9.3 \times 10^{-12}$  s) at 20 °C. This result can be interpreted in terms of an increase of the reorientation rate of water molecules confined inside the micellar core. Similar results were obtained by dielectric measurements on electrolytic solutions [18].

The present paper refers to the low-frequency relaxation processes. The values of the parameters  $\epsilon_1$  and  $\tau_1$  are reported in Figs. 4 and 5, respectively, vs the volume fraction  $\phi$  for each of the investigated series of samples at a fixed NaCl concentration. Both  $\epsilon_1$  and  $\tau_1$  increase monotonically and nonlinearly with  $\phi$  and this dependence is more and more pronounced as NaCl concentration in the micellar aqueous core is reduced. The shape parameter  $a$  keeps approximately constant as  $\phi$  is changed. Typical values of  $a$  around 0.2 have been obtained.

In order to discuss the role of micellar interactions in the dielectric response of these systems we followed the analysis introduced by Van Dijk *et al.* [19]. In particular, the behavior of the complex dielectric constant of water-in-oil microemulsions was explained in terms of the polarizability of the system on introducing an extension of the Clausius-Mossotti equation to higher volume fractions. In fact, for sufficiently dilute suspensions of particles, the Clausius-Mossotti relation gives

$$\alpha = \frac{\epsilon - \epsilon_m}{\epsilon + 2\epsilon_m} = \alpha_p \phi, \quad (2)$$

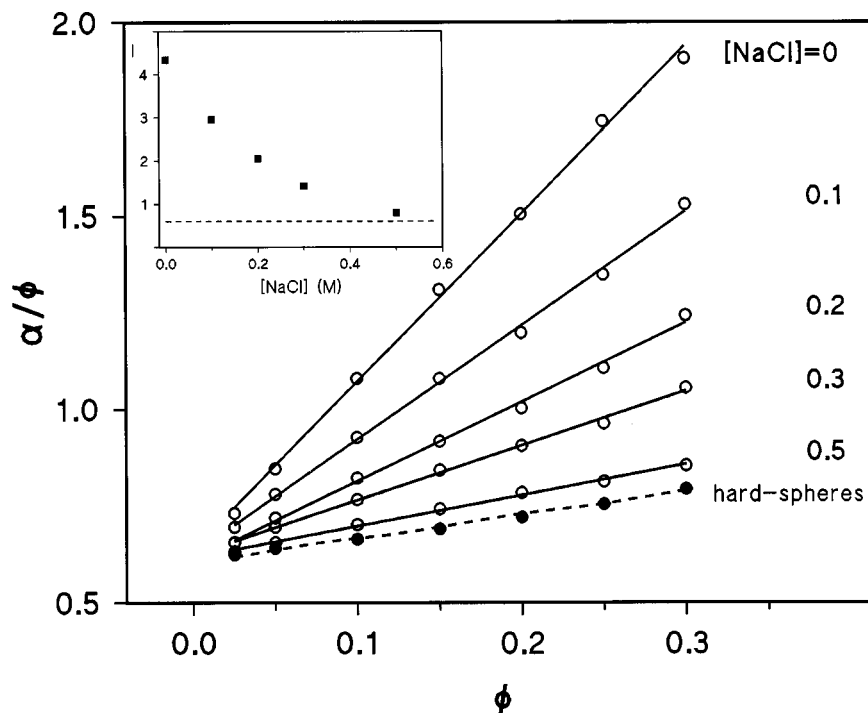


FIG. 6. Ratio of polarizability ( $\alpha$ ) to the volume fraction of the dispersed phase ( $\phi$ ) vs  $\phi$  for samples of microemulsions relative to different concentrations of NaCl brine.  $\circ$ , experimental points;  $\bullet$ , calculated for a hard sphere system (see the text); —, linear fit; - - -, a guide for the eyes. Inset: interaction parameter  $I$  [see Eq. (3)] as a function of NaCl concentration. - - -, value of  $I$  calculated for a hard-sphere suspension.

with  $\epsilon$  the (measurable) permittivity of the samples,  $\epsilon_m$  the permittivity of the continuous oil phase, and  $\alpha_p$  the dipole polarizability per unit volume of a reverse micelle substitute homogeneous sphere of permittivity  $\epsilon_p$  suspended in oil.

If the volume fraction of dispersed particles becomes larger, interactions between the spheres should be accounted for. In fact, if two or more spheres approach each other to a distance comparable to their radius one must take their multipole fields into account in the calculation of the total dipole moment of the cluster of the spheres. If the spheres are conducting or, alternatively, if the dielectric constant inside the spheres is much larger than  $\epsilon_m$ , one finds that the polarizability of such a cluster is enhanced considerably above the value found using only dipole polarizabilities for separate spheres. So when the assumption of independent particles breaks down the average polarizability can be obtained according to the more general expression

$$\alpha = \frac{\epsilon - \epsilon_m}{\epsilon + 2\epsilon_m} = \alpha_p \phi [1 + \phi I(\phi, T)], \quad (3)$$

where  $I(\phi, T)$  gives the correction to Clausius-Mossotti relation.

If the volume fraction is not too large most clusters will be dimers and one expects, in the context of this clustering model [19], that the interaction parameter  $I$  is no longer  $\phi$  dependent, becoming a constant at a fixed temperature. In these conditions a linear behavior of  $\alpha/\phi$  vs  $\phi$  is expected:

The slope of the straight line corresponds to the value of  $I$  and the intercept at  $\phi=0$  to the polarizability of the single particle  $\alpha_p$ .

The  $\alpha/\phi$  values relative to each sample were calculated by replacing the value of  $\epsilon_1$  obtained from fitting the experimental spectra to  $\epsilon$  of Eq. (3). In Fig. 6 the behavior of  $\alpha/\phi$  vs  $\phi$  is shown for all the investigated series of samples relative to different concentrations of NaCl brine. It can be noticed that the experimental values of  $\alpha/\phi$  vs  $\phi$  show a linear trend, suggesting that the clusters present in the examined

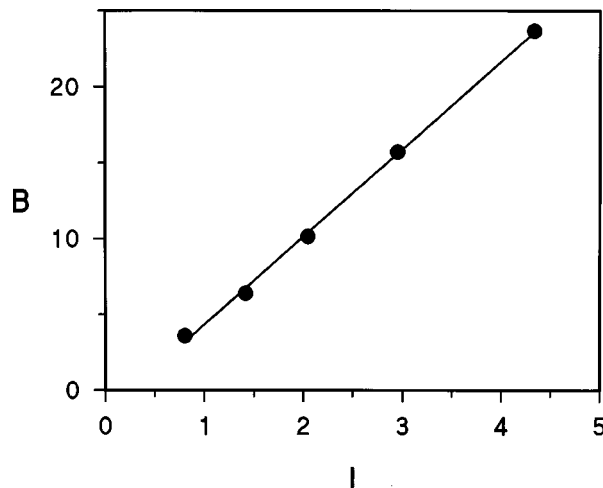


FIG. 7. Plot of  $B$  vs  $I$ . Values of  $B$  were obtained by fitting  $\tau_1$  values according to Eq. (5);  $I$  values were obtained from the slopes of lines in Fig. 3. —, linear fit.

samples are mainly dimers. In order to obtain the values of  $I$  and  $\alpha_p$ , a linear regression procedure has been applied to each series of experimental points. The slope of the best fit lines reported in Fig. 6 decreases as NaCl concentration is increased in the system (see the inset of Fig. 6). These results suggest that dimer formation is more and more hindered for increasing NaCl concentration within the micellar aqueous core. In spite of the strong dependence of  $I$  on salt concentration, the values obtained for  $\alpha_p$  from the different series of measurements do not depend on the amount of NaCl dissolved in the aqueous core. A value of  $\alpha_p$  close to 0.62 is always obtained. According to this result, the addition of NaCl does not affect appreciably the single-particle polarizability.

The decrease in the values of  $I$  on increasing NaCl concentration shows that attractive interactions are progressively lowered by the addition of electrolyte and that the system behaves more and more like a hard-sphere suspension. To obtain further support of this idea, we calculated the values of  $I$  expected for a hard-sphere system. To this aim we used the expression given by Van Djik *et al.* [19]:

$$I = 3R^{-3} \int_0^{\infty} ds s^2 g(s) \left[ \frac{\alpha(s)}{\alpha_p} - 1 \right], \quad (4)$$

where  $R$  is the micellar radius,  $g(s)$  the pair correlation functions for the distribution of the spheres, and  $\alpha(s)$  the dipole polarizability per unit volume of two spheres at a distance  $s$  averaged over the possible orientations of the pair with respect to the electric field. Equation (4) can be evaluated if  $g(s)$  and  $\alpha(s)$  are known. We used for  $g(s)$  the Percus-Yevick hard-sphere pair correlation function and for  $\alpha(s)$  the values for a system of conducting spheres [19]. The values of  $I$  resulting from this procedure together with the experimental value of  $\alpha_p$  were used to calculate the function  $\alpha/\phi$  vs  $\phi$ , for a hard-sphere suspension, by means of Eq. (3). The result is shown in Fig. 6. It can be noticed that, as the concentration of NaCl increases, the behavior of  $\alpha/\phi$  vs  $\phi$  approaches the one calculated for the hard-sphere suspension. This result agrees well with the conclusions of previous neutron scattering [20], light scattering [6], and viscosity [21] measurements on similar systems, suggesting that attractive interactions among the droplets are affected by the addition of electrolyte so that the salted systems behave more like hard-sphere suspensions than their unsalted counterparts.

Attractive interparticle interactions and dimer formation are also expected to influence the dynamical properties of the microaggregates and thus the activation energy of the relaxation is expected to depend on the salt content and  $\phi^2$ . A fitting procedure was applied to the experimental values of  $\tau_1$  vs  $\phi$  by using the equation

$$\tau_1 = \tau_0 e^{B\phi^2}, \quad (5)$$

where  $\tau_0$  is the relaxation time for a noninteracting sphere suspension and  $B$  accounts for the strength of the attractive interactions. Figure 5 shows that Eq. (5) appropriately describes the behavior of  $\tau_1$  vs  $\phi$  for each of the investigated series of samples. The values of  $B$  obtained by the fit decreases with increasing amount of electrolyte in the samples. A correlation is expected between the values of  $B$  as a func-

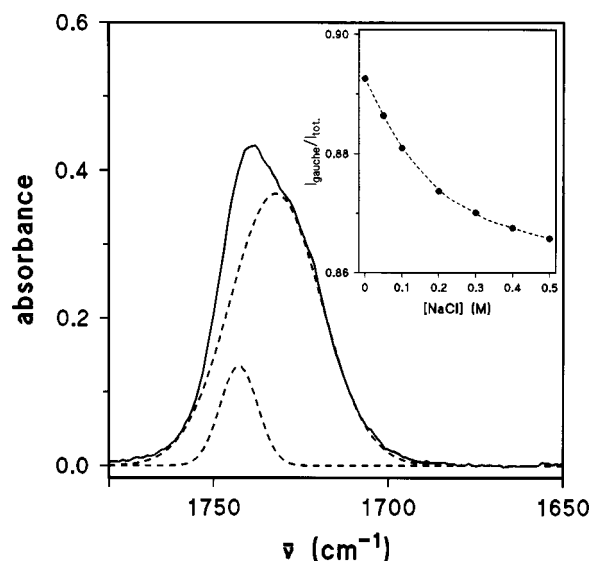


FIG. 8. Infrared absorption spectra of AOT/H<sub>2</sub>O/*n*-heptane systems in the carbonyl stretching frequency region. —, experimental spectrum; - - -, Gaussian components calculated by deconvolution of the experimental spectrum. Inset: ratio between the intensity of the band at lower frequencies assigned to the gauche-like conformer ( $I_{\text{gauche}}$ ) and the intensity of the total carbonyl band ( $I_{\text{tot}}$ ) as a function of NaCl concentration. - - -, a guide for the eyes.

tion of salt concentration and those of the interaction parameter  $I$ . In Fig. 7 the values of  $B$  are plotted as a function of the values of  $I$  obtained from the slopes of lines in Fig. 6. The linear behavior of  $B$  vs  $I$  further supports the proposed description.

## B. Infrared measurements

Figure 8 shows the ir spectra of AOT/H<sub>2</sub>O/*n*-heptane systems at  $W=11$  in the carbonyl stretching mode region (1800–1600 cm<sup>-1</sup>) corrected for the water bending mode contribution (around 1650 cm<sup>-1</sup>). A band around 1730 cm<sup>-1</sup> with an asymmetric shape can be observed. The carbonyl ir

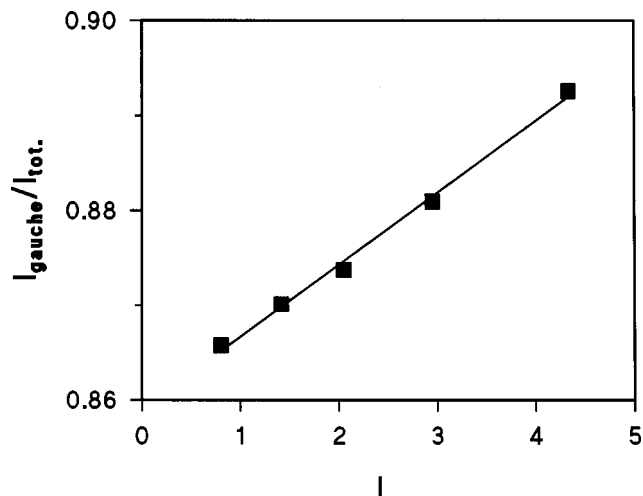


FIG. 9. Values of  $I_{\text{gauche}}/I_{\text{tot}}$  (■) vs values of the interaction parameter  $I$  calculated for the same NaCl concentrations. —, linear fit.

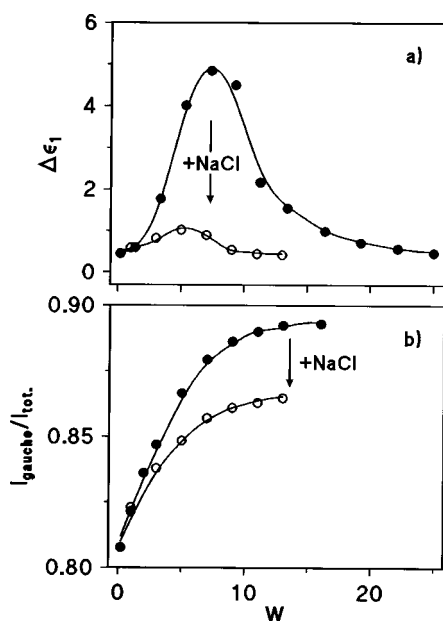


FIG. 10. AOT/H<sub>2</sub>O/*n*-heptane microemulsions ( $\phi=0.2$ ). (a) Relaxation strength  $\Delta\epsilon_1$  and (b) intensity ratio  $I_{\text{gauche}}/I_{\text{tot}}$  vs  $W$ . ●, microemulsions containing H<sub>2</sub>O; ○, microemulsions containing 0.5M NaCl brine. Lines are a guide for the eyes.

band has been reconstructed as a sum of two Gaussian peaks centered at 1738 and 1727  $\text{cm}^{-1}$ . These two Gaussian components arise from a mixture of rotational isomers, with the band at higher frequencies assigned to the translike conformers and the other to the gauche-like conformers [12].

In the inset of Fig. 8 we report the behavior of the ratio between the intensity of the band assigned to the gauche-like conformer and the total carbonyl band as a function of NaCl concentration. It can be noticed that the intensity ratio decreases with increasing salt concentration in the water pool, especially at the lowest salt concentrations. This ratio has been assumed to measure the fraction of gauche-like conformers in the equilibrium mixture. It can be noticed that its value decreases for increasing salt concentration in the water pool, especially at the lowest salt concentrations. This result, which was found not to depend on the volume fraction of dispersed phase, suggests a lower and lower fraction of gauche-like conformers in the equilibrium mixture as NaCl concentration increases. Previous studies [9] showed that these two isomers have different packing factors. In particular, the gauche-like conformer, being the most amphiphilic one with both C=O groups oriented towards the polar side of the surfactant water interface, occupy a larger area per polar head group. We have supposed [3] that the organization of the surfactant polar groups influences the orientation and packing of surfactant chains and, as a consequence, the probability of overlapping between droplets. According to this hypothesis, a correlation is expected between the fractions of AOT gauche-like conformers and the interaction parameter  $I$ , as obtained from dielectric measurements. In Fig. 9 the behavior of the fraction of gauche-like conformers estimated for all the NaCl concentrations considered is plotted versus the interaction parameter  $I$  calculated in the same experimental conditions. A linear behavior can be observed

that lends support to the hypothesis of a direct correlation between the presence of attractive interactions and the composition of the mixture of AOT rotamers.

This hypothesis also provides a possible explanation of the complex shape of variation of the relaxation strength  $\Delta\epsilon_1 = \epsilon_1 - \epsilon_i$  [see Eq. (1)] and  $\tau_1$  vs  $W$  when  $\phi$  is constant, as observed in previous works [2,3] and reported in Fig. 10(a) for the case of the AOT/H<sub>2</sub>O/*n*-heptane system at  $\phi = 0.2$ . In particular, the experimental values of  $\Delta\epsilon_1$  attain a maximum for  $W$  close to 7–8. This maximum, which corresponds to a minimum for the percolation threshold [21], decreases with increasing salinity. Quantities such as conductivity, permittivity, and viscosity show similar behavior [15,21,22].

Figure 10(b) shows that the hydration process of AOT/H<sub>2</sub>O/*n*-heptane microemulsions is accompanied by a change in the profile of the infrared band relative to the carbonyl stretching mode. A gradual increase in  $I_{\text{gauche}}/I_{\text{tot}}$  can be observed up to  $W$  close to 10, related to an increase with  $W$  of the fraction of gauche-like conformers in the equilibrium mixture. Moreover, the value of the intensity ratio  $I_{\text{gauche}}/I_{\text{tot}}$  is significantly reduced when NaCl is added to the samples. These results further support the hypothesis that the attractive intermicellar interactions are favored by a particular orientation and packing of nonpolar tails of AOT molecules in the micellar microaggregate. According to this, the maximum in the permittivity  $\Delta\epsilon_1$  [Fig. 10(a)], conductivity, viscosity, etc., can be explained in terms of the presence of two antagonistic effects connected to the experimental pathway followed here i.e., the change of  $W$  at a fixed value of  $\phi$ . The first effect is a rapid increase of the interaction with  $W$ , correlated to a change in the composition of AOT conformers in the microaggregate. This effect is predominant at low  $W$  values and saturates for  $W > 10$ . The second effect is a decrease of both the number of micellar microaggregates (as  $1/W^3$ ) and their diffusivity connected to the linear increase with  $W$  of the water droplets radius. As a result, the values of  $\Delta\epsilon_1$  pass through a maximum at  $W$  close to 8 and then decrease at larger  $W$  values.

#### IV. CONCLUSIONS

Dielectric spectroscopy and ir data have been used to study the microscopic origin of attractive forces in microemulsions. The experimental pathway followed here, keeping constant the molar ratio and varying the volume fraction of dispersed particles for different concentrations of NaCl, allowed us to obtain quantitative information on the interparticle interaction from the value of the electric permittivity of the sample. A deeper insight into the origin of interactions has been obtained by a comparison of dielectric and ir data. In fact, a strong correlation has been found between the number of AOT gauche-like conformers deduced from the analysis of the carbonyl ir band and the interparticle interaction as deduced by dielectric measurements. This result supports the model proposed by Lemaire, Bothorel, and Roux [5], who attribute the attractive forces among droplets to the possibility of a mutual interpenetration of surfactant tails.

#### ACKNOWLEDGMENT

This work was supported in part by a contribution from the Consiglio Nazionale delle Ricerche (Rome, Italy).

- [1] M. D'Angelo, D. Fioretto, G. Onori, L. Palmieri, and A. Santucci, *Phys. Rev. E* **52**, R4620 (1995).
- [2] M. D'Angelo, D. Fioretto, G. Onori, L. Palmieri, and A. Santucci, *Phys. Rev. E* **54**, 993 (1996).
- [3] M. D'Angelo, D. Fioretto, G. Onori, and A. Santucci, *J. Mol. Struct.* **383**, 157 (1996).
- [4] J. S. Huang, *J. Chem. Phys.* **82**, 480 (1985).
- [5] B. Lemaire, P. Bothorel, and D. Roux, *J. Phys. Chem.* **87**, 1023 (1983).
- [6] B. Bedwell and J. Gulari, *J. Colloid Interface Sci.* **102**, 88 (1984).
- [7] S. Huang, S. A. Safran, M. W. Kim, G. S. Grest, M. Kotlar-chyk, and N. Quirke, *Phys. Rev. Lett.* **53**, 592 (1984).
- [8] A. N. Maitra and H. F. Eicke, *J. Phys. Chem.* **85**, 2687 (1981).
- [9] A. Maitra, *J. Phys. Chem.* **88**, 5122 (1984).
- [10] A. Maitra, G. Vasta, and H. F. Eicke, *J. Colloid Interface Sci.* **93**, 383 (1983).
- [11] H. MacDonald, B. Bedwell, and E. Gulari, *Langmuir* **2**, 704 (1986).
- [12] D. J. Christopher, Y. Yarwood, P. S. Belton, and B. P. Hills, *J. Colloid Interface Sci.* **152**, 465 (1992).
- [13] P. D. Moran, A. Bowmaker, R. P. Cooney, J. R. Bartlett, and J. L. Woolfrey, *Langmuir* **11**, 738 (1995).
- [14] D. Fioretto, A. Marini, M. Massarotti, G. Onori, L. Palmieri, A. Santucci, and G. Socino, *J. Chem. Phys.* **99**, 8115 (1993).
- [15] J. Peyrelasse and C. Boned, *J. Phys. Chem.* **89**, 370 (1985).
- [16] C. Cametti, F. Sciortino, P. Tartaglia, J. Rouch, and S. H. Chen, *Phys. Rev. Lett.* **75**, 569 (1995).
- [17] Y. Feldam, N. Cozlovich, I. Nir, and N. Garti, *Phys. Rev. E* **51**, 478 (1995).
- [18] J. Barthel, H. Hetzenaur, and R. Buchner, *Ber. Bunsenges. Phys. Chem.* **96**, 988 (1992).
- [19] M. A. Van Dijk, J. G. H. Joosten, J. K. Levine, and D. Bedeaux, *J. Phys. Chem.* **93**, 2506 (1989).
- [20] R. Ober and J. Taupin, *J. Phys. Chem.* **84**, 2418 (1980).
- [21] C. Boned and J. Peyrelasse, *J. Surf. Sci. Technol.* **7**, 1 (1991).
- [22] G. Onori and A. Santucci, *Trends Chem. Phys.* **4**, 215 (1996).